

# Freshness-in-Air: An AoI-Inspired UAV-Assisted Wireless Sensor Networks

Chathuranga M. Wijerathna Basnayaka, Dushantha Nalin K. Jayakody\*, Marko Beko

*COPELABS, Lusófona University, Lisbon 1700-097, Portugal*

*Centro de Investigação em Tecnologias - Autónoma TechLab, Universidade Autónoma de Lisboa, Portugal  
Instituto de Telecomunicações, Instituto Superior Técnico, Universidade de Lisboa, 1049-001 Lisbon, Portugal*

---

## Abstract

The Age-of-Information (AoI) metric has emerged as a performance measurement metric for evaluating time-sensitive wireless communications systems. Maintaining the freshness and reliability of data is critical in time-critical wireless networks, where outdated information can have significant consequences. Moreover, short packet transmissions are used in wireless sensor networks (WSNs) to maintain energy efficiency and low latency. This paper proposes a theoretical model that utilizes the AoI metric and finite block length information theory to estimate information freshness in an unmanned aerial vehicle (UAV)-assisted WSN. This network includes multiple sensing nodes and relies on short-packet communication for transmission. In this paper, closed-form expressions for average AoI (AAoI) and the block error rate are derived. Furthermore, the optimal altitude and block length that ensures the freshness of received information at the destination is determined. The results of the analysis provide valuable insights into the performance characteristics of UAV-assisted WSNs and have important implications for the design and optimization of such systems.

*Keywords:* Unmanned Aerial Vehicles (UAV), Age of Information (AoI), Wireless sensor networks, Finite block-length analysis, Short-packet communication.

---

## 1. Introduction

The rapid growth of the Internet-of-Things (IoT), Cyber-Physical Systems, and Unmanned Aerial Vehicle (UAV)-assisted communication networks has unlocked unprecedented opportunities to bolster efficiency across countless domains of our daily lives. Among these, UAV-assisted wireless sensor networks (WSNs) have garnered substantial interest and attention for their potential applications spanning agriculture, disaster relief operations, military endeavours, and beyond [1, 2, 3]. The decisive advantage of employing a UAV-based station in wireless sensor networks lies in its ability to establish reliable line-of-sight (LoS) communication links with ground nodes, thereby mitigating the adverse effects of obstacles and non-line-of-sight (NLoS) conditions that plague traditional terrestrial base stations. By acting as an aerial relay, the UAV can effectively bypass physical obstructions and maintain strong communication links, ensuring timely and reliable data collection from the distributed sensor nodes. This is particularly crucial in urban environments, disaster zones, or terrains where terrestrial infrastructure may be compromised or inaccessible. Moreover, the mobility and flexibility of UAVs enable dynamic adaptation to changing network conditions, allowing for optimal positioning to minimise communication delays [4]. In time-critical

WSN applications where prompt and accurate information is of the essence, maintaining the freshness and reliability of data acquires paramount importance, as outdated or stale information can precipitate severe and far-reaching consequences. Traditional performance metrics like latency and delay, however, prove inadequate in providing a comprehensive understanding of the timeliness of data, thereby failing to fully capture its freshness.

To overcome this shortcoming, the Age-of-Information (AoI) concept has emerged as a novel and innovative metric to quantify the freshness of information. AoI is defined as the time elapsed since the generation of the last successfully received update at the destination, capturing the timeliness and relevance of the data. By focusing on the age of the latest update, AoI provides a comprehensive understanding of the information freshness, taking into account both the generation and the successful delivery of updates. [5, 6, 7]. The AoI metric furnishes valuable insights into the effectiveness of time-sensitive systems such as UAV-assisted WSNs, thereby serving as a potent tool for evaluating their performance in time-critical applications [8, 9, 10]. While existing works have analysed AoI for single-source or grant-based protocols in URLLC-enabled UAV networks [4, 11, 12], they have largely overlooked the challenges posed by multi-source scenarios that are prevalent in practical WSN deployments. Notably, in real-world WSN environments, multiple sensing nodes often coexist and transmit data simultaneously, leading to potential collisions, interference, and degradation of information freshness. Failing to account for these multi-source dynamics can result in inaccurate

---

\*Corresponding author

*Email addresses:* a22201874@alunos.ulht.pt  
(Chathuranga M. Wijerathna Basnayaka),  
dushantha.jayakody@ulusofona.pt (Dushantha Nalin K. Jayakody),  
beko.marko@ulusofona.pt (Marko Beko)

estimates of system performance and suboptimal resource allocation, ultimately compromising the effectiveness of the WSN in time-critical applications [13].

The paper addresses the pivotal problem of analysing the Average Age of Information (AAoI) for UAV-assisted WSNs with multiple sensing nodes. A novel theoretical framework is developed that synergistically combines the AoI metric with finite block-length information theory to estimate information freshness in such multi-source UAV-WSN settings under short-packet transmissions. The key motivations are two-fold: 1) to bridge the gap in existing literature by extending AoI analysis to realistic multi-source UAV-WSN scenarios, and 2) to leverage finite block-length information theory principles in multi-source UAV-WSN scenarios, which are better suited for analysing short-packet communications compared to traditional information-theoretic approaches that assume infinitely long block lengths. By adopting a finite block-length analysis, the work accounts for the practical constraints of short-packet transmissions that are commonly employed in WSNs to conserve energy and maintain low latency.

The main contributions of this work are as follows:

- Developed a theoretical model that synergistically combines the Age of Information (AoI) metric and finite block-length information theory to estimate information freshness in a UAV-assisted WSN comprising multiple sensing nodes and employing short-packet communication.
- Derived closed-form expressions for the average AoI (AAoI) and block error rate in the considered multi-source UAV-assisted WSN.
- Determined the optimal UAV altitude, block length, and sensor activation probability that minimises the AAoI and ensures the freshness of received information at the destination node.
- Formulated a lemma that specifies the optimal sensor activation probability required to maintain an optimal AoI at the destination, and validated its efficacy and correctness through comprehensive simulations.
- Demonstrated through simulations that the proposed UAV-assisted WSN significantly outperforms traditional fixed base transceiver station (BTS)-based systems in maintaining information freshness, particularly in urban scenarios where the performance gap is substantial.

By addressing the crucial problem of multi-source AoI analysis for UAV-WSNs, this paper provides valuable insights into the design and optimisation of such systems, paving the way for more reliable and efficient time-critical WSN applications leveraging UAVs. Notably, our work holds significant promise for a wide array of real-world applications, ranging from smart city monitoring and management to disaster response and relief efforts, where ensuring the timely availability of up-to-date information is of paramount importance for informed decision-making and effective resource allocation. In smart city scenarios, for instance, UAV-assisted WSNs can enable efficient

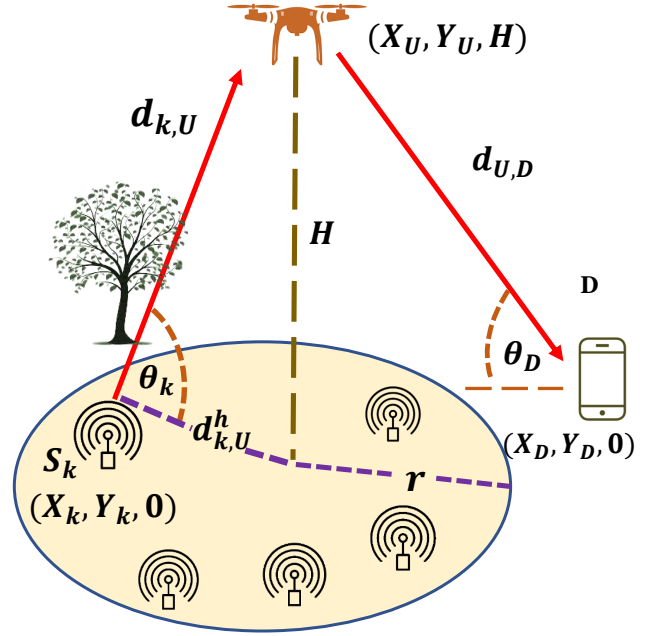


Figure 1. System model of UAV-assisted WSN: A UAV at altitude  $H$  serving as a decode-and-forward relay between sensor nodes  $S_k$  and the destination node  $D$ .

monitoring of traffic patterns, air quality, noise levels, and energy consumption, thereby facilitating data-driven urban planning and resource management. Similarly, in the aftermath of natural disasters or emergencies, our proposed framework can help emergency responders collect accurate and timely information, enabling them to make informed decisions and allocate resources optimally, ultimately saving lives and minimising the devastating impacts of such events.

By providing a comprehensive theoretical analysis of information freshness in multi-source UAV-WSNs, our work not only advances the state-of-the-art in this domain but also serves as a foundation for future research endeavours aimed at further enhancing the performance and reliability of these systems. Ultimately, our contributions underscore the critical importance of accounting for multi-source dynamics and leveraging innovative information-theoretic approaches in the design and optimisation of UAV-assisted WSNs, paving the way for a future where these systems can realise their full potential in enabling a wide range of time-critical applications that demand timely and accurate information.

The remaining sections of this paper are organized as follows: Section 2 presents the system model and evaluates the block error rate and the AAoI of the network. Section 3 presents numerical simulation results and evaluates the performance of the system. Finally, Section 4 summarizes the conclusions drawn in the paper.

## 2. System Model

As shown in Fig. 1, we consider a UAV-assisted WSN, where the UAV ( $U$ ) is placed at an altitude of  $H$  and it acts

as a wireless decode-and-forward (DF) relay between the sensor nodes ( $S_k \forall k \in \{1, \dots, K\}$ ) and the destination (D) node. Suppose that each ground node  $S_k$  has a fixed location  $L_k = (X_k; Y_k; 0)$  and the location of the UAV and Destination are denoted as  $L_U = (X_U; Y_U; H)$  and  $L_D = (X_D; Y_D; 0)$  respectively. The horizontal distance between each node  $i$  and  $j$  is  $l_{i,j} = \sqrt{(X_i - X_j)^2 + (Y_i - Y_j)^2}$  where  $i \in (S_k, U), j \in (U, D)$ . The  $S_k$  is said to be in the coverage of the UAV if their horizontal distance  $l_{k,U}$  is less than or equal to  $r$ . The elevation angle of UAV is  $\theta_k$  and if it is measured from the  $S_k$ ,  $\theta_k = \tan^{-1}(\frac{H}{l_{k,U}})$  and if it is measured from the  $D$ ,  $\theta_D = \tan^{-1}(\frac{H}{l_{U,D}})$ . In this wireless communication system, the transmission time is divided into equal intervals known as time blocks. Each time block is further divided into two slots and each slot is used to transmit a single packet. Each sensor node in the network becomes active independently with a probability of  $P_{a,j}$  at the beginning of each block and the probability follows a binomial distribution with parameters  $(K; P_{a,j})$ . The system does not consider any feedback or re-transmission policies, which means that each update is delivered only once. In the first slot, sensor nodes send data to the UAV relay, and all sensor nodes share the same wireless resources. In the second slot, the UAV decodes and transmits the data to the destination. There is no direct communication between the sensor nodes and the destination.

The system considers both line-of-sight (LoS) and non-line-of-sight (NLoS) links between the UAV and the ground stations (sensor nodes or destination). The probability of LoS between the UAV and ground station  $l \in (S_k, D)$  can be expressed as follows [14, 11]:

$$P_{\text{LoS}}(\theta_l) = \frac{1}{1 + \rho \exp(-\varphi(\theta_l - \rho))}, \quad (1)$$

where  $\rho$  and  $\varphi$  are S-curve parameters that are completely dependent on the environment. The large-scale channel gain  $\alpha$  for the channel between transmitting node  $i \in (S_k, U)$  and receiving node  $j \in (U, D)$  is determined as follows [11]:

$$-10 \log(\alpha_{ij}) = 20 \log(d_{i,j}) + 20 \log\left(\frac{4\pi f_{c,i,j}}{c}\right) + \eta_{\text{NLoS}} \quad (2) \\ + \frac{\eta_{\text{LoS}} - \eta_{\text{NLoS}}}{1 + \rho \exp(-\varphi(\theta_l - \rho))},$$

where  $f_{c,i,j}$  and  $c$  are the carrier frequency (Hz) and the speed of the light (m/s), respectively.  $\eta_{\text{NLoS}}$  and  $\eta_{\text{LoS}}$  are the expectations of the additional environment-dependent excessive path loss for the LoS and NLoS components, respectively. Assuming that the three nodes remain static during transmission and ignore the Doppler effect, we employ the Rician fading model to investigate the small-scale channel characteristics and multi-path propagation in this system<sup>1</sup>. The probability distribution of small-scale channel gain ( $g_{ij}$ ) follows a non-central chi-square distribution, and the probability density function<sup>2</sup>

<sup>1</sup>The small-scale channel gain is denoted as  $g_{ij} = |H_{ij}^2|$ , where  $H_{ij}$  represents the Rician fading channel coefficient.

<sup>2</sup> $F_X(x)$  and  $f_X(x)$  represents the cumulative distribution function (CDF) and probability density function (PDF) of an arbitrary random variable  $X$ , respectively.

for the small-scale channel gain can be expressed as:

$$f_{g_{ij}}(z) = \frac{(K_L + 1) e^{-K_L} e^{-\frac{(K_L+1)z}{\bar{g}_{ij}}}}{\bar{g}_{ij}} I_0 \left( 2 \sqrt{\frac{K_L(K_L+1)z}{\bar{g}_{ij}}} \right), \quad (3)$$

where  $z \geq 0$ ,  $\bar{g}_{ij} = 1$ ,  $I_0(\cdot)$  is the zero-order modified Bessel function of the first kind, and  $K_L$  is the Rician factor, which can be expressed as follows [15, 11]:

$$K_L = \frac{P_{\text{LoS}}(\theta_l)}{1 - P_{\text{LoS}}(\theta_l)} = \frac{1}{\rho \exp(-\varphi(\theta_l - \rho))}. \quad (4)$$

Then, the instantaneous signal-to-noise ratio (SNR) at each receiving node can be calculated as follows:

$$\gamma_j = \frac{\alpha_{ij} g_{ij} P_i}{\sigma^2}, \quad (5)$$

where  $\alpha_{ij}$  is the large-scale channel gain,  $g_{ij}$  is the small-scale channel gain,  $P_i$  is the transmission power at node  $i$  and  $\sigma^2$  is the noise power at the receiver. In addition, the expectation of SNR at the node  $j$  can be calculated as the function of  $l_{i,j}$  as follows:

$$\bar{\gamma}_j(l_{i,j}) = \frac{D e^{\frac{A}{1 + \rho \exp(-\varphi(\tan^{-1}(\frac{H}{l_{i,j}}) - \rho))}}}{\left(l_{i,j}^2 + H^2\right)}, \quad (6)$$

where  $A = \frac{-(\eta_{\text{LoS}} - \eta_{\text{NLoS}}) \ln(10)}{10}$  and  $D = \frac{P_i 10^{-\frac{G}{10}}}{\sigma^2}$ , where  $G = 20 \log\left(\frac{4\pi f_{c,i,j}}{c}\right) + \eta_{\text{NLoS}}$ . Furthermore, the conditional PDF of SNR at the UAV is given by:

$$f_{\gamma_{k,U}}(z | l_{k,U}) = \frac{(K_L + 1) e^{-K_L} e^{-\frac{(K_L+1)z}{\bar{\gamma}_{k,U}}}}{\bar{\gamma}_{k,U}} I_0 \left( 2 \sqrt{\frac{K_L(K_L+1)z}{\bar{\gamma}_{k,U}}} \right). \quad (7)$$

Thus,  $F_{\gamma_{k,U}}(z, | l_{k,U})$  can be derived as in [16]:

$$F_{\gamma_{k,U}}(z, | l_{k,U}) = 1 - Q_1 \left( \sqrt{2K_L}, \sqrt{\frac{2(K_L+1)z}{\bar{\gamma}_{k,U}}} \right), \quad (8)$$

where  $Q_1(\cdot, \cdot)$  is first order Marcum Q-function. However, due to the intricate complexity of the Marcum Q-function, an approximation is utilized as in [17] at the high SNRs in order to derive a closed-form equation for  $F_{\gamma_{k,U}}(z | l_{k,U})$  as follows:

$$F_{\gamma_{k,U}}(z, | l_{k,U}) \approx \frac{e^{-K_L} (1 + K_L) z}{\bar{\gamma}_{k,U}}. \quad (9)$$

Furthermore,  $F_{\gamma_{k,U}}(z)$  can be formulated as follows:

$$F_{\gamma_{k,U}}(z) = \int_0^\infty F_{\gamma_{k,U}}(z | l_{k,U}) f_{l_{k,U}}(l_{k,U}) dl_{k,U}, \quad (10)$$

where  $f_{l_{k,U}}(l_{k,U})$  can be calculated as follows, since it is assumed that sensor nodes are uniformly distributed:

$$f_{l_{k,U}}(l_{k,U}) = \begin{cases} \frac{2l_{k,U}}{r^2}, & l_{k,U} \leq r, \\ 0, & \text{otherwise.} \end{cases} \quad (11)$$

Moreover, (10) can be reformulated as follows using (6), (9), (10) and (11) :

$$F_{\gamma_{k,U}}(z) = \frac{2}{Dr^2} \int_0^r \frac{e^{-\frac{W_l}{1-W_l}z} (l_{k,U}^2 + H^2) l_{k,U}}{\underbrace{(1-W_l) e^{AW_l}}_{q_l(l_{k,U},z)}} dl_{k,U}, \quad (12)$$

where  $W_l = \frac{1}{1+\rho \exp(-\varphi(\tan^{-1}(\frac{H}{l_{k,U}})-\rho))}$ . Then, since the Gaussian-Chebyshev Quadrature method converges much faster than other approximation methods, it has been employed for the integration of  $q_l(l_{k,U}, z)$  to obtain a closed-form expression for (13) as follows [18]:

$$F_{\gamma_{k,U}}(z) = \frac{2}{Dr} \sum_{m=1}^M \frac{M}{\pi} \sqrt{1-\phi_m^2} q_l(\alpha_l, z) + R_M, \quad (13)$$

where  $\phi_m = \cos\left(\frac{2m-1\pi}{M}\right)$ ,  $\alpha_l = \frac{r}{2}\phi_m + \frac{r}{2}$ ,  $M$  is the complexity-accuracy trade-off factor.  $R_M$  is the error term, and at high  $M$  values,  $R_M$  becomes negligible and has little impact on the overall system performance. Furthermore, the CDF of  $\gamma_{U,D}$  can be expressed as in [16] :

$$F_{\gamma_{U,D}}(z) = 1 - Q_1\left(\sqrt{2K}, \sqrt{\frac{2(K+1)z}{\bar{\gamma}_{U,D}}}\right), \quad (14)$$

where  $Q_1(\cdot, \cdot)$  is the first-order Marcum Q-function, a function that is challenging to manipulate directly [19]. Thus, a semi-linear approximation is employed to derive a closed-form expression for  $F_{\gamma_{U,D}}(z)$  as in [19, 11]:

$$\begin{aligned} F_{\gamma_{U,D}}(z) &\simeq \Psi\left(\sqrt{2K}, \sqrt{\frac{2(K+1)z}{\bar{\gamma}_{U,D}}}\right), \\ &\simeq \Psi(\omega_1, \omega_2), \end{aligned} \quad (15)$$

where  $\Psi(\omega_1, \omega_2)$  is the semi-linear approximation of the  $1 - Q_1(\omega_1, \omega_2)$  and it can be calculate as in [19].

### 2.1. Block Error Probability

In order to analyze block error probability using finite block length information theory, it is assumed that fading coefficients remain constant throughout each transmission block. In addition, it is assumed that the receiver possesses accurate channel state information. Consequently, the expectation of decoding error probability at each receiving node is expressed as follows [20]:

$$\varepsilon_j = \mathbb{E} \left[ Q \left( \frac{n_{i,j} (\log_2(1 + \gamma_j)) - k_b}{\sqrt{n_{i,j} \left( \frac{\log_2^2 e}{2} \left( 1 - \frac{1}{(1 + \gamma_j)^2} \right) \right)}} \right) \right], \quad (16)$$

where  $\mathbb{E}[\cdot]$  denotes the expectation operator and  $Q(x) = \frac{1}{\sqrt{2\pi}} \int_x^\infty e^{-\frac{t^2}{2}} dt$ . It is assumed that  $k_b$  information bits are contained in a  $n_{i,j}$  bit length block. Moreover, under the Rician

fading block fading conditions,  $\varepsilon_j$  can be expressed as

$$\varepsilon_j = \int_0^\infty f_{\gamma_j}(z) Q \left( \frac{n_{i,j} (\log_2(1 + \gamma_j)) - k_b}{\sqrt{n_{i,j} \left( \frac{\log_2^2 e}{2} \left( 1 - \frac{1}{(1 + \gamma_j)^2} \right) \right)}} \right) dz. \quad (17)$$

Obtaining a closed-form expression for the overall decoding error probability can be challenging due to the complexity of the Q-function. To address this matter, an approximation technique similar to the approach in [21, 11] has been used as follows:

$$\varepsilon_j \approx \beta_j \sqrt{n_{i,j}} \int_{\phi_j}^{\delta_j} F_{\gamma_j}(z) dz \simeq F_{\gamma_j}(\psi_j). \quad (18)$$

where  $\beta_j = \frac{1}{2\pi \sqrt{2^{\frac{2k_b}{n_{i,j}}} - 1}}$ ,  $\psi_j = 2^{\frac{k_b}{n_{i,j}}} - 1$ ,  $\phi_j = \psi_j - \frac{1}{2\beta_j \sqrt{n_{i,j}}}$  and  $\delta_j = \psi_j + \frac{1}{2\beta_j \sqrt{n_{i,j}}}$ . Then, using (13), (15) and (18) closed form expression for block error at each node can be derived. The probability of a node successfully updating the UAV at the end of the first time slot, denoted by  $\tau_{k,U}$ , occurs when a node transmits during the slot, no other node transmits, and the UAV correctly decodes the packet. Then,  $\tau_{k,U}$  can be calculated as follows:

$$\tau_{k,U} = P_{a,k} (1 - \varepsilon_{k,U}) \prod_{k \neq j} (1 - P_{a,j}). \quad (19)$$

Then, the overall decoding error probability can be expressed as  $\varepsilon_{ovr,k} = 1 - \tau_{k,U} + \varepsilon_{U,D} \tau_{k,U}$  [21].

### 2.2. Age of Information Analysis

The AAoI at the  $D$  for update each node  $S_k$  is computed as follows, using [11]:

$$\Delta_k^{AAoI} = \frac{\mathbb{E}[X_k^2]}{2\mathbb{E}[X_k]} + T, \quad (20)$$

where  $X_k$  denotes the inter-departure time between two consecutive successfully received status updates at  $D$ . It assumes that the end-to-end delay of each successfully received update is always a constant, this is given by  $T = (n_{k,U} + n_{U,D}) T_s$ , where  $T_s$  is the symbol duration. The inter departure time  $X_k$  is a geometric random variable with mean  $\mathbb{E}[X_k] = \frac{T}{1 - \varepsilon_{ovr,k}}$  and second moment  $\mathbb{E}[X_k^2] = \frac{2T^2}{(1 - \varepsilon_{ovr,k})^2} - \frac{T^2}{1 - \varepsilon_{ovr,k}}$ . Then, (20) can be reformulated as follows:

$$\Delta_k^{AAoI} = T \left( \frac{1}{2} + \frac{1}{1 - \varepsilon_{ovr,k}} \right). \quad (21)$$

Finally, the network AAoI can be calculated as follows [22]:

$$\Delta_{net}^{AAoI} = \frac{T}{2} + \frac{T}{K} \sum_{k=1}^K \frac{1}{1 - \varepsilon_{ovr,k}}. \quad (22)$$

**Lemma 1.** The optimal value for the active probability of sensors that minimizes  $\Delta_{net}^{AAoI}$  is  $P_{a,k}^* \approx \frac{1}{K}$ .

**Proof:** It is assumed that in networks comprising numerous nodes, node  $k$  is likely to have a small optimal active probability  $P_{a,k}^*$ . Then, using inequality  $1-y \leq e^{-y}$  and  $1-y \approx e^{-y}$  for small  $y$ , (19) can be reformulated as follows:

$$\tau_{k,U} \leq \frac{P_{a,k}(1-\varepsilon_{k,U})}{(1-P_{a,k})} e^{-\sum_{j=1}^K P_{a,j}}. \quad (23)$$

Then,  $\hat{\Delta}_{net}^{AAOI}$  the lower bound of  $\Delta_{net}^{AAOI}$  can be calculated as

$$\Delta_{net}^{AAOI} \geq \hat{\Delta}_{net}^{AAOI} = \frac{T}{2} + \frac{T e^{\sum_{j=1}^K P_{a,j}}}{K} \sum_{k=1}^K \frac{1}{\Phi_k} \left( \frac{1}{P_{a,k}} - 1 \right), \quad (24)$$

where  $\Phi_k = (1-\varepsilon_{k,U})(1-\varepsilon_{U(k),D})$ . Then, defining the quantities as

$$A = \sum_{k=1}^K \frac{1}{\Phi_k} \left( \frac{1}{P_{a,k}} - 1 \right) \text{ and } A' = \sum_{k=1}^K \frac{1}{\Phi_k P_{a,k}}, \quad (25)$$

the first-order optimality conditions for  $\hat{\Delta}_{net}^{AAOI}$  can be calculated as  $P_{a,k} = \frac{1}{\sqrt{A\Phi_k}}$ . As in (25),  $A < A'$  and as a result,  $P_{a,k}^*$  can be derived as follows:

$$P_{a,k} \geq \frac{1}{A'\Phi_k P_{a,k}} = \frac{\sqrt{A\Phi_k}}{A'\Phi_k} = \frac{1/\sqrt{\Phi_k}}{\sum_{j=1}^K (1/\sqrt{\Phi_k})} \approx \frac{1}{K} \approx P_{a,k}^*. \quad (26)$$

### 3. SIMULATION RESULTS

In this section, numerical results are presented to validate the theoretical derivations. Unless otherwise specified, the simulation parameters are set as  $r = 400$  m,  $d_{U,D} = 1000$  m,  $H = 500$  m,  $f_{c_{s,U}} = 900$  MHz,  $f_{c_{U,D}} = 2.4$  GHz,  $c = 3 \times 10^8$  ms<sup>-1</sup>,  $\eta_{LOS}$  (Suburban) = 0.1 dB,  $\eta_{NLOS}$  (Suburban) = 21 dB,  $\eta_{LOS}$  (Urban) = 1 dB,  $\eta_{NLOS}$  (Urban) = 20 dB,  $\eta_{LOS}$  (Dense urban) = 1.6 dB,  $\eta_{NLOS}$  (Dense Urban) = 23 dB,  $\eta_{LOS}$  (High-rise urban) = 2.3 dB,  $\eta_{NLOS}$  (High-rise Urban) = 34 dB,  $P_{S_k} = 90$  mW,  $P_U = 0.2$  W,  $T_s = 17$   $\mu$ s,  $n_{k,U} = 54$  bits,  $n_{U,D} = 54$  bits,  $k_b = 32$  bits,  $P_a = 0.2$ ,  $K = 5$  nodes and  $\sigma^2 = -100$  dBm [15].

In Fig. 2, the network AAOI is plotted against the altitude of the UAV using (22). The results indicate that the optimal altitude is 600 m in all environmental conditions. At lower altitudes, the network AAOI is higher due to the high error probability caused by the weak LoS. As altitude increases towards the optimal value, the AAOI decreases rapidly due to a stronger LoS that outweighs the impact of path loss. However, beyond the optimal altitude, the path loss dominates other factors, leading to a higher network AAOI. When the altitude is between 250 m - 700 m, the network AAOI is at its minimum for all environments except for high-rise urban. The network AAOI cannot be reduced to its minimum due to a low SNR caused by weak LoS conditions in high-rise urban areas. The suburban environment has the lowest AAOI for all altitudes due to strong channel conditions.

Fig. 3 shows the impact of block length on network AAOI in this system. Longer block lengths increase system delay as

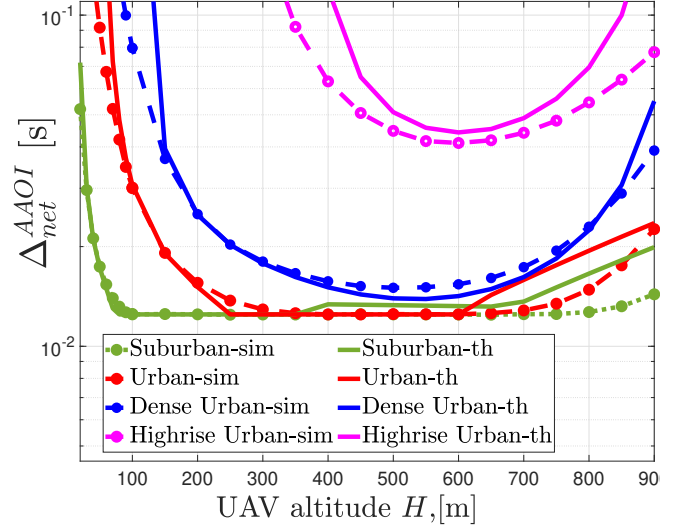


Figure 2. Network AAOI as a function of UAV altitude for different environments.

transmission time directly correlates with block length. Conversely, shorter block lengths result in more decoding errors. For smaller block lengths, decoding error probability significantly affects AAOI compared to transmission time. However, when the block length increases towards its optimal value, AAOI decreases due to fewer decoding errors. Beyond optimal value, the increase in transmission time outweighs the reduction in transmission errors, resulting in a higher AAOI. Therefore, when selecting the block length in a wireless communication system, it is important to balance the trade-offs between transmission time and decoding error to ensure optimal AAOI performance of the system.

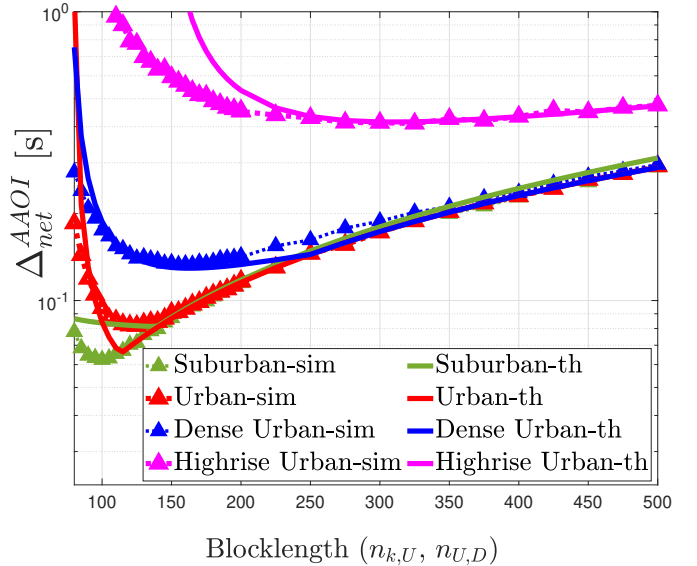


Figure 3. Network AAOI as a function of Blocklength for different environments.

Fig. 4 illustrates the relationship between the network AAOI and the active probability ( $P_a$ ) for different numbers of nodes.

As illustrated in the figure, a small active probability results in a higher network AAOI due to the scarcity of frequent status updates at the destination. As the active probability increases towards its optimal point, the AAOI decreases due to more frequent updates at the destination. However, beyond the optimal value, increasing the active probability increases the network AAOI due to a higher number of transmission collisions. Notably, Fig. 4 highlights that the system achieves the minimum network AAOI when  $P_a \approx 1/K$ , as stated in Lemma 1.

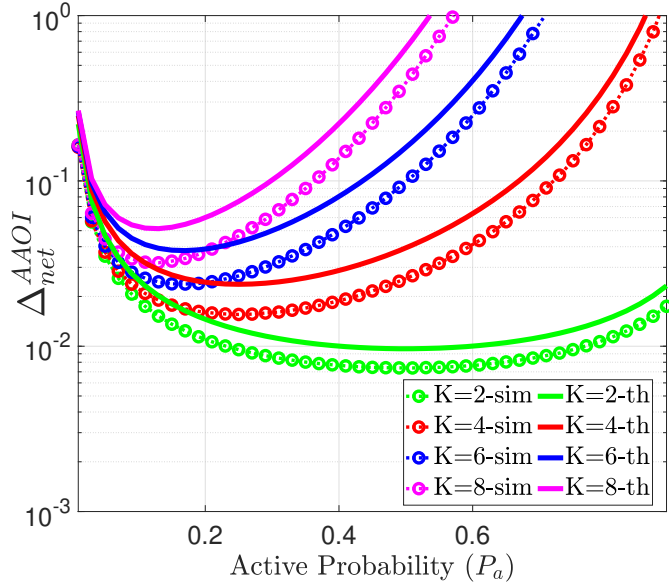


Figure 4. Network AAOI as a function of Active Probability ( $P_a$ ) for different numbers of nodes ( $K$ ) in a wireless network.

Fig. 5 illustrates the relationship between network AAOI and total transmission power for the UAV-assisted WSN and traditional fixed BTS-based system under different environmental conditions. As shown, transmission power significantly impacts AAOI, with AAOI decreasing as transmission power increases in both scenarios. However, in the UAV-assisted WSN model, AAOI remains nearly constant beyond 0.1W due to the low transmission error rate at the receiver. The UAV-assisted WSN significantly improves information freshness compared to the traditional fixed terrestrial-based BTS-assisted WSN, with a larger performance gap in urban scenarios. The proposed UAV-assisted WSN model better maintains information freshness in WSNs under various environmental conditions, particularly in dense urban areas where traditional fixed BTS-based systems fail due to poor LoS conditions. This makes the model suitable for real-world urban applications, such as smart city scenarios and disaster management. In smart cities, UAV-assisted WSNs enable efficient monitoring of traffic, air quality, noise levels, and energy consumption. In disaster management, the model ensures accurate and up-to-date information collection, enabling informed decision-making and effective resource allocation by emergency responders, ultimately saving lives in the aftermath of natural disasters or emergencies.

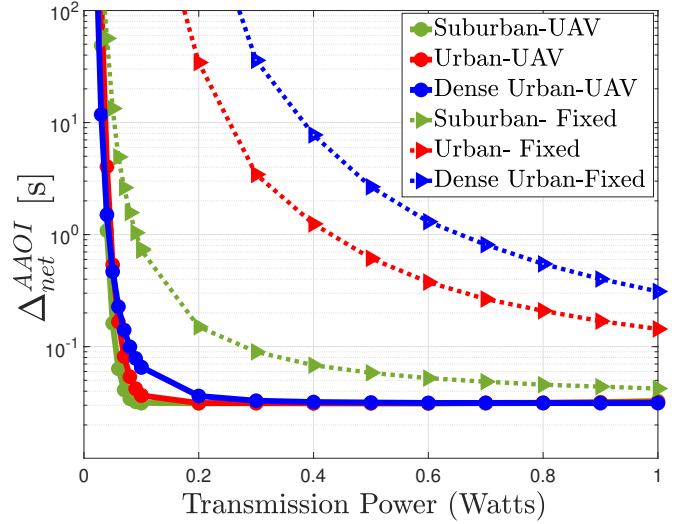


Figure 5. Network AAOI vs. total transmission power for UAV – assisted and fixed BTS– based WSNs under different environments.

#### 4. Conclusion

This paper presents a study on the freshness of data in a UAV-assisted WSN with multiple sensors, using AoI as a metric. Closed-form expressions for the network AAOI and block error probability, which depend on the UAV altitude, block length, and activation probability of sensors, have been derived. Our numerical analysis reveals the existence of an optimal block length, UAV altitude, and activation probability that minimizes the network AAOI, thus ensuring the freshness of the sensor network. Both theoretical analysis and simulation results demonstrate that the optimal activation probability that minimizes the network AAOI. This approximately equals the reciprocal of the number of nodes in the network. Furthermore, the simulation results clearly show that the proposed UAV-assisted WSN system significantly outperforms the traditional fixed-BTS based system in terms of maintaining the freshness of information. The proposed system model navigates the system designers in allocating communication resources for UAV-assisted WSNs and designing more reliable and efficient WSN systems in practical applications. While this study focuses specifically on UAV-assisted WSNs, integrating edge servers with WSN systems also could further enhance the freshness of the information. Future research should explore how this type of system enhances the freshness of the information and conduct a comparative analysis between the UAV-based solution and the edge server-based solution to provide valuable insights into the optimal design of WSN systems.

#### Acknowledgments

This work was supported, in part, by the COFAC - Cooperativa de Formação e Animação Cultural, C.R.L. (University of Lusófona University) via the project PortuLight (COFAC/ILIND/COPELABS/2/2023), by the national funds through FCT - Fundação para a Ciência e a Tecnologia

- as part the project AIEE-UAV(no. 2022.03897.PTDC), CEECINST/00002/2021/CP2788/CT0003 and COPELABS (no. UIDB/04111/2020) and by the European Commission via Marie Skłodowska-Curie Actions (MSCA) as part of the project REMARK-ABLE (No. 101086387).

## Conflict of interest

The authors declare that there is no conflict of interest in this paper.

## References

- [1] A. A. Laghari, A. K. Jumani, R. A. Laghari, and H. Nawaz, "Unmanned aerial vehicles: A review," *Cogn. Robot.*, vol. 3, pp. 8–22, 2023.
- [2] H. Nawaz, H. M. Ali, and A. A. Laghari, "Uav communication networks issues: A review," *Arch. Comput. Methods Eng.*, vol. 28, no. 3, pp. 1349–1369, 2021.
- [3] A. A. Khan, A. A. Laghari, T. R. Gadekallu, Z. A. Shaikh, A. R. Javed, M. Rashid, V. V. Estrela, and A. Mikhaylov, "A drone-based data management and optimization using metaheuristic algorithms and blockchain smart contracts in a secure fog environment," *Comput. Electr. Eng.*, vol. 102, no. C, sep 2022.
- [4] J. Wang, L. Bai, Z. Fang, R. Han, J. Wang, and J. Choi, "Age of information based urllc transmission for uavs on pylon turn," *IEEE Trans. Veh. Technol.*, pp. 1–14, 2024.
- [5] S. Liyanaarachchi and S. Ulukus, "The role of early sampling in age of information minimization in the presence of ack delays," *IEEE Trans. Inf. Theory*, pp. 1–1, 2024.
- [6] C. M. W. Basnayaka, D. N. K. Jayakody, T. D. P. Perera, T. T. Hämäläinen, and M. Marques Da Silva, "Age of information in a swipt and urllc enabled wireless communications system," in *Proc. IEEE Int. Conf. Adv. Netw. and Tele. Syst.*, 2022, pp. 302–307.
- [7] C. M. W. Basnayaka, D. N. K. Jayakody, T. D. P. Perera, and M. Beko, "Dataage: Age of information in swipt-driven short packet iot wireless communications," *IEEE Internet of Things J.*, pp. 1–1, 2024.
- [8] X. Gao, X. Zhu, and L. Zhai, "Aoi-sensitive data collection in multi-uav-assisted wireless sensor networks," *IEEE Trans. Wirel. Commun.*, pp. 1–1, 2023.
- [9] T. D. P. Perera, D. N. K. Jayakody, I. Pitas, and S. Garg, "Age of information in swipt-enabled wireless communication system for 5gb," *IEEE Wireless Commun.*, vol. 27, no. 5, pp. 162–167, 2020.
- [10] Y. Emami, H. Gao, K. Li, L. Almeida, E. Tovar, and Z. Han, "Age of information minimization using multi-agent uavs based on ai-enhanced mean field resource allocation," *IEEE Trans. Veh. Technol.*, pp. 1–14, 2024.
- [11] C. M. W. Basnayaka, D. N. K. Jayakody, and Z. Chang, "Age of information based URLLC-enabled UAV wireless communications system," *IEEE Internet Things J.*, 2021.
- [12] X. Zhang, J. Wang, and H. V. Poor, "Aoi-driven statistical delay and error-rate bounded qos provisioning for murllc over uav-multimedia 6g mobile networks using fbc," *IEEE J. Sel. Areas Commun.*, vol. 39, no. 11, pp. 3425–3443, 2021.
- [13] A. Munari, "Modern random access: An age of information perspective on irregular repetition slotted aloha," *IEEE Trans. Commun.*, vol. 69, no. 6, pp. 3572–3585, 2021.
- [14] A. Al-Hourani, S. Kandeepan, and S. Lardner, "Optimal lap altitude for maximum coverage," *IEEE Commun. Lett.*, vol. 3, no. 6, pp. 569–572, 2014.
- [15] B. Wang, J. Ouyang, W.-P. Zhu, and M. Lin, "Optimal altitude of uavs for minimum boundary outage probability with imperfect channel state information," in *Proc. IEEE/CIC Int. Conf. Commun. China (ICCC)*. IEEE, 2019, pp. 607–611.
- [16] D. Mishra, S. De, and D. Krishnaswamy, "Dilemma at rf energy harvesting relay: Downlink energy relaying or uplink information transfer?" *IEEE Trans. Wireless Commun.*, vol. 16, no. 8, pp. 4939–4955, 2017.
- [17] A. Gil, J. Segura, and N. M. Temme, "Algorithm 939: Computation of the marcum q-function," *ACM Trans. Math. Softw.*, vol. 40, no. 3, pp. 1–21, 2014.
- [18] M. Abramowitz, I. A. Stegun, and R. H. Romer, "Handbook of mathematical functions with formulas, graphs, and mathematical tables," 1988.
- [19] H. Guo, B. Makki, M.-S. Alouini, and T. Svensson, "A semi-linear approximation of the first-order marcum q-function with application to predictor antenna systems," *IEEE Open J. Commun. Soc.*, vol. 2, pp. 273–286, 2021.
- [20] G. Durisi, T. Koch, J. Östman, Y. Polyanskiy, and W. Yang, "Short-packet communications over multiple-antenna rayleigh-fading channels," *IEEE Trans. Commun.*, vol. 64, no. 2, pp. 618–629, 2015.
- [21] Y. Gu, H. Chen, Y. Li, and B. Vucetic, "Ultra-reliable short-packet communications: Half-duplex or full-duplex relaying?" *IEEE Wirel. Commun.*, vol. 7, no. 3, pp. 348–351, 2017.
- [22] R. D. Yates and S. K. Kaul, "Status updates over unreliable multiaccess channels," in *Proc. IEEE Int. Symp. Inf. Theory*, 2017, pp. 331–335.